

AN ADAPTIVE QRS DETECTION ALGORITHM WITH VARIABLE THRESHOLD

خوارزم تكيفي للتعرف على الـ QRS
باستخدام مشرف متغير

*
Fatma E.Z. Abou-Chadi and Manal M.I. Saleh **

* Department of Electrical Communications
Faculty of Engineering - Mansoura University

** Mansoura Electronic Exchange

الخلاصة - تتعرض تسجيلات رسم القلب لكمية كبيرة من الشوشرة الناتجة من مصادر مختلفة مثل النشاط العضلي ،
ازاحة خط الأساس نتيجة للتنفس ، حركة العريض والأجهزة الالكتروميكانيكية . وفي هذا البحث نعرض تقنية للتعرف
على مواضع موجات الـ QRS في وجود كمية كبيرة من الشوشرة ، ويعتمد الخوارزم على حساب عدد من المتغيرات
الإحصائية وتعيين حد (مشرف) تكيفي لإزالة رسم القلب ما يساعد على تتبع التغيرات التي تحدث في خط الأساس
للاشارة وبالتالي يحسن من حساسية التعرف على مواضع الـ QRS .

ABSTRACT- Ambulatory electrocardiogram (ECG) recordings from patients undergoing severe physical stress are corrupted by large muscle artifacts (EMG) and other noise sources, such as baseline drifts and currents induced by motion artifacts and electromechanical devices. A simple real-time algorithm has been developed which is suitable for on-line detection of the QRS complexes. The algorithm calculates several statistical parameters of the ECG signal which are used to adapt the threshold to baseline changes in the signal, thereby increasing detection sensitivity.

1. INTRODUCTION

In recent years the trend toward automated analysis of electrocardiograms (ECG) has gained momentum. Many systems have been implemented in order to perform such tasks as 12-lead off-line electrocardiogram analysis, Holter tape analysis, and real time monitoring. An important issue in the analysis of ECG's is the monitoring of occurrence times of near-periodic events of particular phenomena. The major area of monitoring lies in the study of heart rate variability, i.e., the spontaneous fluctuations in the heart rate, by means of the reliable identification and location of the most prominent feature of the ECG, the QRS complex.

Under normal conditions, in the absence of muscle artifacts and other electrical perturbations, a large signal-to-noise ratio (SNR) prevails. The techniques involved in the detection of the QRS complex have long been established with varying degrees of success. However, in some applications, such as ergonomics, a patient may undergo severe physical stress. The ECG signal will be corrupted with a large nonstationary stochastic muscle artifact signal together with extraneous transient and continuous noise components due to motion artifacts and electromechanical devices. The SNR, in this case, will be very much reduced and may often be inferior to unity. Under such circumstances most QRS complex detection techniques fail [1].

The existing algorithms for QRS detection can be classified into four categories: algorithms based on both fixed amplitude threshold and first derivative [2-4], algorithms that use first derivative only [5], algorithms utilizing both first and second derivative [6], and algorithms employing digital filters [7-12]. However, many of these algorithms require a relatively noise-free digitized ECG. Data corrupted with noise must either be filtered or discarded. ECG quality assurance not only requires human or software noise detection schemes, but also may result in the loss of clinically significant data. This is an important design consideration for applications in real-time heart monitoring.

Algorithms based on amplitude and slope have a significant advantage as they are most immune to electromyographic interference. However, these algorithms are sensitive to changes in baseline which accounts for the decrease in performance. If changes in baseline can be corrected by high pass filtering and/or a cubic spline, these algorithms would offer the highest performance [13]. However, these operations can alter the signal and may require substantial computations.

In this paper, we propose a simple real-time QRS detection algorithm which can be used under both reduced- and large- nonstationarity conditions. The algorithm is based on the determination of an adaptive variable threshold and the first derivative. It calculates several statistical parameters of the ECG signal, which are used on-line to adapt the algorithm to the nature of the signal.

The performance of the proposed algorithm is compared with three other algorithms using a database consisted of a synthesized normal ECG (used as a gold standard) corrupted with five types of synthesized noise.

2. THE QRS DETECTION ALGORITHM

It is already known that a detection algorithm based on a fixed threshold and first derivative faces two problems. These are as follows:

1) If one selects a small value for the threshold then in addition to the true QRS complexes, all types of single-peaked waves having high magnitude will be detected e.g. T-wave, P-wave, and other artifacts.

2) If one selects a large value for the threshold, then the algorithm will not identify all types of QRS complexes and QRS waves with small amplitudes will be missed.

We are proposing a real-time algorithm, which on-line calculates some statistical parameters of the signal to be analysed, and adapts itself to the nature of the signal by recalculating the threshold value at each sample. The proposed algorithm optimizes the tradeoff between high performance in case of high frequency noise and the insensitivity to changes in baseline. The threshold is not constant, and depends on the nature of the signal.

The proposed detection algorithm consists of the following steps:

Step 1: The algorithm takes a moving window of length N samples from the raw electrogram data. Denote this sequence by X_i ($i = 1, 2, \dots, N$). The algorithm calculates the following

The described detection algorithm is presented in Fig.1. In the inner loop, the algorithm recursively calculates the statistical parameters, calculates the time derivative, and updates the threshold value while $X_k < T_k$ and no change in the sign of y_k . When the conditions are not met, the algorithm saves the pair (X_k, k) and enters the next detection cycle.

; DETECTION ALGORITHM

statistical parameters for each N sample points centered at the kth sample:

1) Mean value \bar{X}_k , defined as

$$\bar{X}_k = \frac{1}{N} \sum_{i=k-m}^{k+m} X_i, \quad (1)$$

$$N = 2m + 1$$

2) Standard deviation σ_k , defined as

$$\sigma_k = \sqrt{\frac{1}{N} \sum_{i=k-m}^{k+m} (X_i - \bar{X}_k)^2} \quad (2)$$

3) Third moment M_k , defined as

$$M_k = \left[\frac{1}{N} \sum_{i=k-m}^{k+m} (X_i - \bar{X}_k)^3 \right]^{1/3} \quad (3)$$

The standard deviation σ of the signal indicates the deviation of the sample from the mean value. It is a good measure to distinguish the low-variability signal regions from the high-variability signal regions. In some cases, however, the standard deviation is not good enough as a measure to detect short variations [14]. Therefore, the algorithm calculates the third moment and uses it as an additional criterion for calculating the threshold.

Step 2: A threshold value T_k is calculated for each sample using the formula:

$$T_k = C_1 X_k + C_2 \sigma_k + C_3 M_k \quad (4)$$

where C_1 , C_2 , and C_3 are constants to be determined empirically.

Step 3: The difference y_i between two successive samples X_i and X_{i+1} is formed, such that

$$y_i = X_{i+1} - X_i \quad (5)$$

If $X_i > X_{i+1}$, y_i is negative, indicating that a downslope exists.

the ECG for a total of 32 s. Following the procedure reported by Friesen et al. [13], the digitized ECG was subsequently edited until it appeared consistent with the analog recording and stored in a Fortran data file as a linear array of 8192 single precision floating-point numbers. The heart rate is a constant 69 beats per minute, the QRS width is 80 ms and the R-wave amplitude is 1.08 mV. A plot of a segment of the uncorrupted ECG is shown in Fig.2.

B- The simulated signal

We have chosen five types of noise and we have developed their models for simulation using the methods reported by Friesen et al. [13]. These are:

- 1) electromyographic interference (EMG),
- 2) powerline interference,
- 3) baseline drift due to respiration,
- 4) abrupt shifts in the baseline, and
- 5) motion artifacts
- 6) a composite of all of the above.

We did not simulate other types of noise such as electrosurgical and instrumentation noise as they behave similarly to the random model used for EMG.

Each of the six types of noise is added to an uncorrupted ECG at four different levels: 25, 50, 75, and 100 percent of the maximum amplitude.

1) **Electromyographic Interference:** This type of noise is simulated by adding random noise to the ECG. The maximum noise level is formed by adding random numbers derived from a zero-mean Gaussian distribution of +50 percent of the ECG maximum amplitude to the uncorrupted signal. The reduced noise levels are formed by scaling the random numbers by appropriate amount. A plot of the ECG corrupted by electromyographic noise is given in Fig.3.

2) **Powerline Interference:** Fifty Hertz noise is generated using sine function generator. The maximum noise level corresponds to a peak-to-peak amplitude of 0.333 mV. A plot of the ECG corrupted with powerline noise is shown in Fig.4. Harmonic powerline frequencies were not modelled since the 50 Hz component is dominant.

3) **Baseline Drift Due to Respiration:** This type of interference is simulated by adding a low frequency sinusoid to the uncorrupted ECG. The frequency is 0.333 Hz and the maximum amplitude is 1.0 mV peak. It is generated in the same manner as the powerline interference using different amplitude and frequency. Amplitude effects due to respiration were not modeled. A plot of the ECG corrupted by baseline drift due to respiration is illustrated in Fig.5.

4) **Abrupt Shift in Baseline:** This type of interference represents an abrupt shift in baseline due to movement of the patient while the ECG is being recorded. It is simulated by adding a dc bias for a given segment of the ECG. The maximum noise level consists of six alternating baseline shifts of +0.5 or -0.5 mV. This resulted in five baseline shifts of +1.0 or -1.0 mV and one of +0.5 mV. Fig.6 shows a plot of the ECG corrupted by abrupt shifts in baseline.

In reality, shifts in ECG baselines are less abrupt than our model; hence we are performing a worst case simulation for the amplitude-slope QRS algorithms.

5) Motion Artifacts: Motion artifacts are transient baseline changes caused by changes in the electrode-skin impedance with electrode motion. The usual cause of motion artifacts will be assumed to be vibrations or movements of the subject. It is simulated by adding a low frequency sine wave to the uncorrupted signal. The maximum amplitude is 4.32 mV peak and the frequency is 0.1 Hz. Fig.7 illustrates the ECG corrupted by motion artifacts.

6) Composite Noise: A composite noise is formed by combining all of the noise types described above. The maximum noise level is constructed by reducing the maximum noise level of each type of noise to 50 percent of the maximum and then summing them. The reduced noise levels of the composite are formed by scaling the constructed composite noise and then adding it to the uncorrupted ECG. Fig.8 shows a plot of the resultant ECG.

4. THE EVALUATION CRITERIA

Hamilton and Tompkins proposed criteria for evaluation of QRS detectors [15]. When a QRS complex occurs, a detection algorithm either indicates or fails to indicate the event. Proper detection of a valid QRS complex represents a true-positive (TP) event. Missing a valid QRS complex represents a false-negative (FN) event. Similarly a false-positive (FP) event is an indication of a detection in the absence of any QRS complex. Multiple detection (MD) occurs when the QRS detector triggers more than once within the same QRS window.

Our scoring algorithm compares the onset of the QRS candidate to a key file containing the locations of all of the valid QRS onsets. If the candidate onset falls between the actual onset and the end of the QRS complex (a window of 22 sample points or 88 ms was chosen), it is scored as a QRS detection. If the candidate onset occurs outside these boundaries, it is counted as a false positive. The percentage of QRS complexes correctly detected is calculated at the end of each run by dividing the number of QRS complexes correctly detected by the total number of actual QRS complexes.

Since the search for the next QRS complex resumes at the next point following the candidate onset, it is possible that the same QRS complex will be detected more than once. Only the first correct detection will be included in the scoring of QRS-complexes found or the measure of delay. Subsequent detections which fall within the boundaries of the first detected QRS were classified as multiple detection (MD).

An indication of the time delay (TD) required for detection is also calculated after each run. If the detection occurs after the actual onset but before the end of the QRS complex, it is classified as a late detection. The number of sample points between the onset and the detection are summed for all of the detections of that run.

5. RESULTS

The results of the application of the described detection method with variable threshold are listed in Tables I-IV. Each table gives the results of one level for the six types of noise. The values of the constants C_1 , C_2 , and C_3 in Eq.(4) were determined by varying each constant independently until

the algorithm gave the best results when the ECG was corrupted by a 100 percent composite noise. These were found to be $C_1 = 0.9$, $C_2 = 0.71$, and $C_3 = 0.71$. Fig.9 shows the corrupted ECG signal with composite noise (solid line) and the determined threshold T_k calculated using Eq. (4) (dashed line). Note that the threshold always follows the baseline movement.

Table I Detection results using the uncorrupted ECG

TP	FP	FN	MD	TD	% QRS (Detected)
37	0	0	0	0	100

Table II Detection results using the 50% noise level

Noise Type	TP	FP	FN	MD	TD	% QRS (detected)
EMG	37	0	0	0	5	100
Powerline	37	0	0	0	0	100
Respiration	37	0	0	0	0	100
Baseline drift	37	0	0	0	0	100
Motion	37	0	0	0	0	100
Composite	37	0	0	0	1	100

Table III Detection results using the 75% noise level

Noise Type	TP	FP	FN	MD	TD	% QRS (detected)
EMG	37	0	0	0	7	100
Powerline	37	0	0	0	13	100
Respiration	37	0	0	0	0	100
Baseline drift	37	0	0	0	0	100
Motion	37	0	0	0	0	100
Composite	37	0	0	0	4	100

Table IV Detection results using the 100% noise level

Noise Type	TP	FP	FN	MD	TD	% QRS (detected)
EMG	37	0	0	0	12	100
Powerline	37	0	0	0	13	100
Respiration	37	0	0	0	0	100
Baseline drift	37	0	0	0	0	100
Motion	37	0	0	0	0	100
Composite	37	0	0	0	8	100

We compared the proposed method with three other algorithms using slope and fixed threshold criteria [2]-[4]. The percentage of correct detection obtained for the fixed threshold methods ranges from 81.1 to 91.9 percent for the 100 percent noise corrupted ECG. The proposed variable threshold algorithm gives as high as 100% correct detection which is a good compromise.

Table V evaluates the number of TP, FP, FN and the time delay (TD) in QRS detection for the three fixed threshold algorithms and the proposed method in case of composite noise. The table indicates that our algorithm optimizes the tradeoff between the high performance in case of large baseline movements and the accurate detection in the presence of high frequency noise.

Table V Comparison of Four Algorithms
(Composite Noise 100% level)

Algorithm	TP	FP	FN	TD	% QRS (Detected)
Moriet-Mahoudeaux [2]	31	0	6	25	83.8
Fraden-Neuman [3]	33	22	6	37	81.1
Gustafon [4]	34	1	3	1	91.9
Proposed Algorithm	37	0	0	8	100

6. CONCLUSION

We presented an adaptive real-time algorithm for on-line detection of the QRS complexes. The algorithm reliably detects QRS complexes using some statistical parameters to adjust automatically the threshold so that it adapts to variations in the baseline of the ECG signal, thereby increasing the detection sensitivity. Its effectiveness can be attributed to its insensitivity to baseline changes as well as its accurate performance in case of high frequency noise. The most significant result is that no sharp jump of baseline has been

misclassified as QRS-complex. So, this algorithm is very robust to baseline wandering.

REFERENCES

- [1] O. De Vel. R-wave Detection in the presence of muscle artifacts. IEEE Trans Biomed. Eng., **BME-31**, 715-717, (1984).
- [2] P.M. Mahoudeaux et al. Simple microprocessor-based system for on-line ECG analysis. Med. Biol. Eng. Comput., **19**, 497-500, (1981).
- [3] J. Fraden and M. R. Neuman. QRS wave detection. Med. Biol. Eng. Comput., **19**, 125-132, (1980).
- [4] D. Gustafson et al. Automated VCG interpretation studies using signal analysis techniques. R-1044 Charles Stark Draper Lab., Cambridge, MA, (1977).
- [5] W. P. Holsinger et al. A QRS preprocessor based on digital differentiation. IEEE trans. Biomed. Eng., **BME-18**, 212-217, (1971).
- [6] M. L. Ahlstrom and W. J. Tompkins. Automated high-speed analysis of holter tapes with microcomputers. IEEE trans. Biomed. Eng., **BME-30**, 651-657, (1983).
- [7] C. S. Weaver et al. Digital filtering with applications to electrocardiogram processing. IEEE Trans. Audio Electroacoust., **AU-16**, 350-389, (1968).
- [8] M. Okada. A digital filter for the QRS complex detection. IEEE Trans. Biomed. Eng., **BME-26**, 700-703, (1979).
- [9] Chung-Shyan et al. A nonlinear digital filter for QRS-complex detection. Proc. of the IEEE/seventh Ann. Conf. of the Eng. in Medicine and Biol. Society, 845-848, (1985).
- [10] J. Pan and W. J. Tompkins. A real-time QRS detection algorithm. IEEE Trans. Biomed. Eng., **BME-32**, 230-236, (1985).
- [11] M. L. Ahlstrom and W. J. Tompkins. Digital filters for real-time ECG signal processing using microprocessors. IEEE Trans. Biomed. Eng., **BME-32**, 708-713, (1985).
- [12] J. A. van Alste and T. S. Schilder. Removal of base-line wander and power-line interference from the ECG by an efficient FIR filter with a reduced number of taps. IEEE trans. Biomed. Eng., **BME-32**, 1052-1060, (1985).
- [13] G. M. Friesen et al. A comparison of the noise sensitivity of nine QRS detection algorithms. IEEE Trans. Biomed. Eng., **BME-37**, 85-98, (1990).
- [14] B. Furht and A. Perez. An adaptive real-time ECG compression algorithm with variable threshold. IEEE Trans. Biomed. Eng., **BME-35**, 489-494, (1988).
- [15] P. S. Hamilton and W. S. Tompkins. Evaluation of QRS detection algorithms using the IBM PC. Proc. of the IEEE/seventh ann. Conf. of the Eng in Med. and Biol. Society, 830-833, 1985.

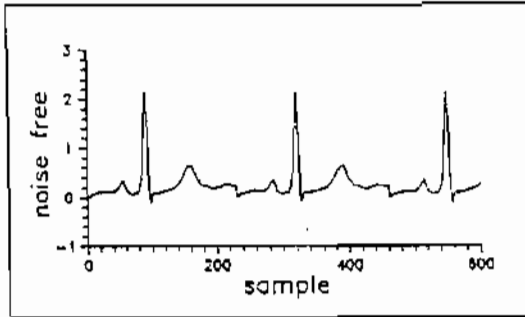


Fig.2 The uncorrupted ECG

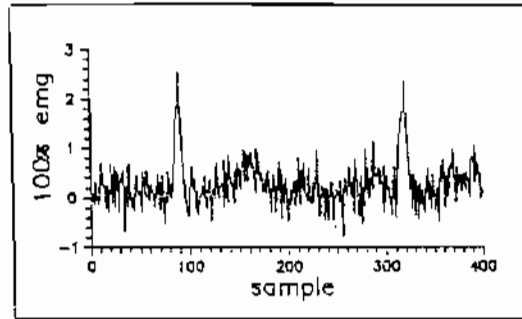


Fig.3 ECG corrupted with EMG noise

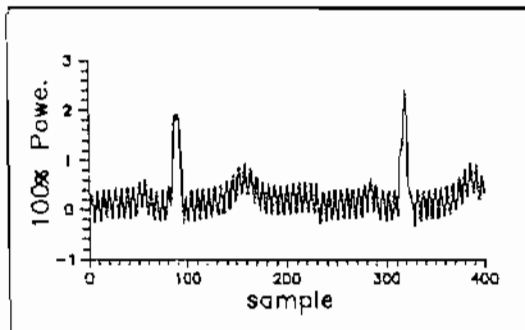


Fig.4 ECG corrupted with powerline interference

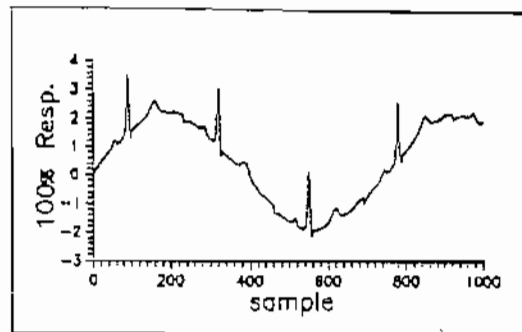


Fig.5 ECG corrupted with respiration

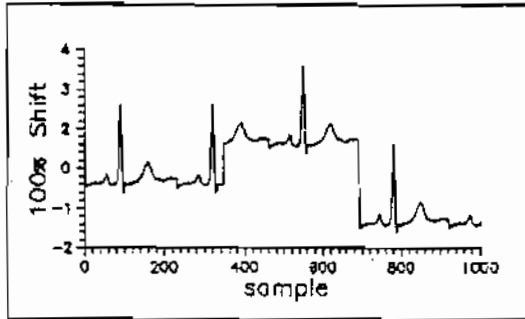


Fig.6 ECG corrupted with baseline drift

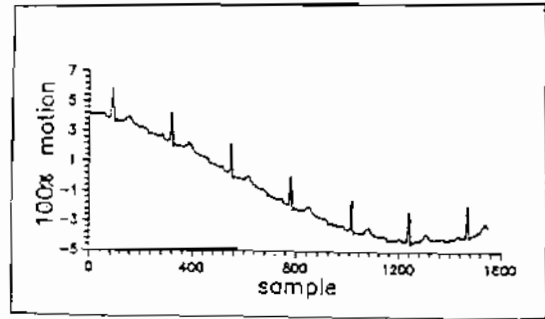


Fig.7 ECG corrupted with motion artifacts

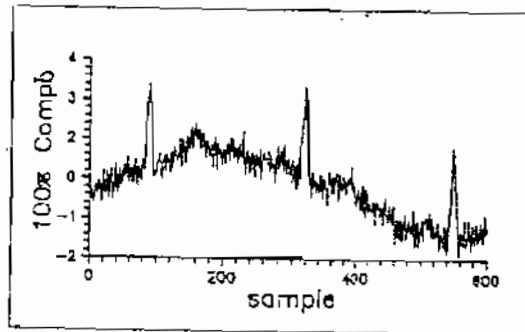


Fig.8 ECG corrupted with composite noise

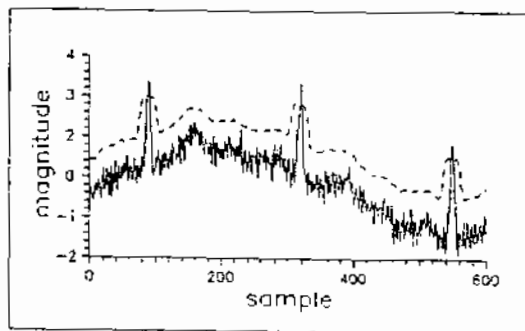


Fig.9 An illustrative example of the QRS detection procedure.
 (a) ECG corrupted with 100 percent composite noise (—)
 (b) The calculated variable threshold (- - -)